Microstructural and hardness behavior of graphene-nanoplatelets/aluminum composites synthesized by mechanical alloying

R. Pérez-Bustamante, D. Bolaños-Morales, J. Bonilla-Martínez, I. Estrada-Guel, **R. Martínez-Sánchez**

Abstract

Graphene can be considered as an ideal reinforcement for the production of composites due to its outstanding mechanical properties. These characteristics offer an increased opportunity for their study in the production of metal matrix composites (MMCs). In this research, the studied composites were produced by mechanical alloying (MA). The employed milling times were of 1, 3 and 5 h. GNPs were added in 0.25, 0.50 and 1.0 wt% into an aluminum powder matrix. Milled powders were cold consolidated and subsequently sintered. Composites were microstructurally characterized with Raman spectroscopy and electron microscopy and X-ray diffraction. The hardness behavior in composites was evaluated with a Vickers micro-hardness test. A homogeneous dispersion of graphene during MA and the proper selection of sintering conditions were considered to produce optimized composites. The obtained results with electron microscopy indicate a homogeneous dispersion of GNPs into the aluminum matrix. Analyses showed GNPs edges where the structure of the graphene layers conserved after MA is observed.

1. Introduction

The wide application of aluminum in the automotive and aerospace industry, makes of aluminum-matrix composites an important option to meet future challenges in the design of structural components. In this concern, the reinforcement material

used in the production of composites plays a key role in order to maximize the mechanical performance of the composites. The use of nanometric reinforcement materials for the development of aluminum-matrix composites has demonstrated a positive effect on the mechanical behavior of the final products. This has been the case of aluminum-matrix composites reinforced with carbon nanotubes (CNTs) [1]; [2] ; [3] and most recently reinforced with graphenes [4] ; [5]. A single layer of graphite is called graphene and has extraordinary electrical, thermal, and physical properties. The nanometric nature and high specific surface area allow a great interaction of reinforcement phase with the matrix even in small concentrations.

Even when the effect of CNTs in the microstructure and mechanical properties in aluminum-matrix composites is being widely investigated nowadays [6] ; [7], the development of graphene/aluminum composites has attracted the attention of several research groups [4] ; [5]. This is due to the outstanding mechanical properties that graphene offers, and because they have an important effect on aluminum-based composites improving the mechanical behavior. In this regard, graphene can be produced in single or multiple layers. It has also been possible to produce large areas of graphenes [8] under controlled conditions. However, the production of composites with future automotive and aerospace applications implies the use of greater amounts of material than the provided by the synthesis techniques used in the production of a large area of graphene layers. In this regard, graphene nanoplatelets (GNPs) comprise multiple graphene sheets with a stack-like morphology, having an important fraction of the mechanical properties of

individual graphene layers [9], which make them excellent potential nanofillers in the production of aluminum-matrix composites.

The use of GNPs in the production of composites, with improved mechanical properties, involves achieving a homogeneous dispersion of the filler into the matrix. Several methods for an effective dispersion of nanoparticles have been the result of powder metallurgy routes. Additionally, dispersion methods based on mechanical milling technique increase the effectiveness in the dispersion of the filler in the matrix [10] ; [11].

In this research, the use of GNPs in the production of GNP/Al composites is investigated. The use of several milling times and GNP concentration, as well as the selection of sintering time in the production of composites have been considered.

2. Experimental procedure

Aluminum powder (99.9% pure, −325 mesh in size) and GNPs produced from graphite exfoliation were used as the starting materials to produce GNP/Al composites. Fig. 1 shows a secondary electron micrograph obtained from field emission scanning electron microscopy (FESEM, JEOL model JSM-7401F) of the stack-like morphology of GNPs. Graphene sheets of less than 10 nm in thickness are observed. GNPs and Al powder were placed in a vial made from a hardened steel tool and milling media made from a hardened stainless steel. The production of composites was made by mechanical milling (MM) in a high energy ball mill Spex 8000 M. GNPs were added in several compositions (0.0, 0.25, 0.50 and 1.0 wt%). The identification codes of each composite as function of the GNP concentration and milling time are shown in Table 1. The powder mass was 8.5 g and the ball-to-

powder ratio was set to 5:1. All milling runs were performed with methanol as a process control agent (PCA) and argon atmosphere to avoid excessive agglomeration and oxidation, respectively. The milling times were of 1, 3 and 5 h. Milled powders were cold consolidated to form discs of 6.7 mm of diameter and 1 mm of height, under ~950 MPa and then sintered under Ar atmosphere during 0.5, 1, 2, 3, 4, and 5 h at 500 °C with a heating and cooling rate of 5 °C/min. A non-milled Al sample was prepared under the same conditions. The morphology evolution and microstructure of the as-milled powders were studied by scanning electron microscopy (SEM) in a JEOL model JSM-5800LV. Additional observations were carried out in composites after sintering process by SEM. Changes in the crystallinity of the as-milled GNP/Al composite powders as function of milling were followed by Raman spectroscopy with a Micro Raman LabRAM VIS-633 with an He–Ne laser light (632.8 nm). X-ray diffraction (XRD, Panalytical X'Pert PRO with X'Celerator detector, interval 20–80°) analysis was used to study the phase crystallization occurred during the sintering process. Sintered products were imaged with a transmission electron microscopy (TEM) in a JEOL model JEM 2200FS. Specimens for TEM were prepared by focusing ion beam (FIB) in a JEOL model JEM-9320FIB. The hardness behavior was evaluated with the Vickers micro-hardness test. The hardness test conditions were 200 g of load and 15 s of dwell time. The average value of at least 10 indentations in each sample is reported.

3. Results

Raman spectroscopy was used to characterize the effect of milling time in the structure of GNP. Fig. 2 compares the variation in Raman spectra for GNP/Al

powders milled in a high energy ball mill as a function of milling time. The Raman spectra of the 1D composite is shown at the top of the figure, whilst in the bottom the 5D composite is presented. The existence of GNPs in the aluminum matrix can be corroborated in Fig. 2. Raman spectra of the composites presents the characteristic signals of multilayer graphene with peaks corresponding to the D (1333 cm^{-1}), G (1583 cm^{-1}) and 2D band (2670 cm^{-1}). The intensity of the peaks is reduced as the milling time increases. This indicates an increase in the amorphous fraction of the GNPs as a function of milling time. The effect of mechanical milling on carbon structure such as graphite, diamond

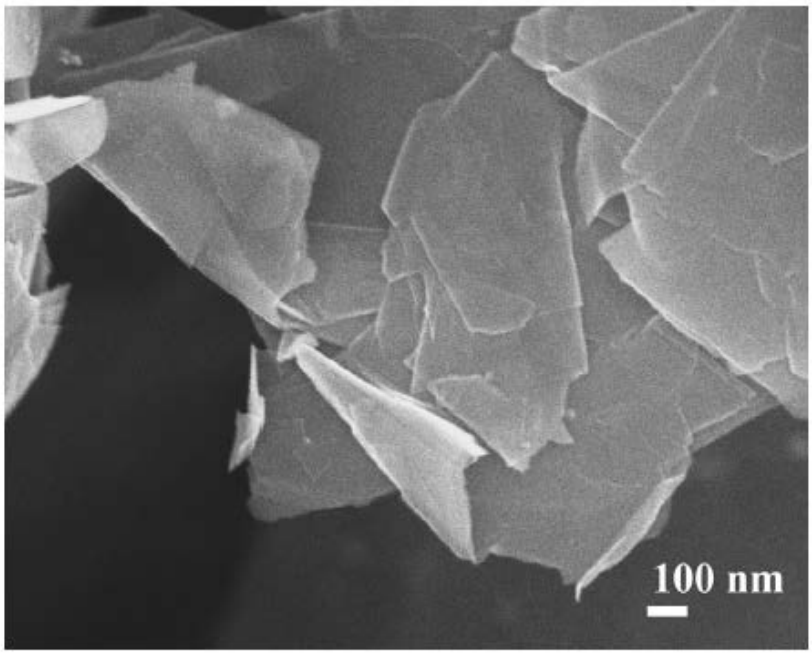

Fig. 1. Secondary electron FESEM micrograph of the multilayered morphology of graphene nanoplatelets.

Table 1
Composite identification.

Milling time (h)	GNP concentration (wt%)			
	0	0.25	0.5	1.0
1	1A	1B	1C	1D
3	3A	3B	3C	3D
5	5A	5B	5C	5D

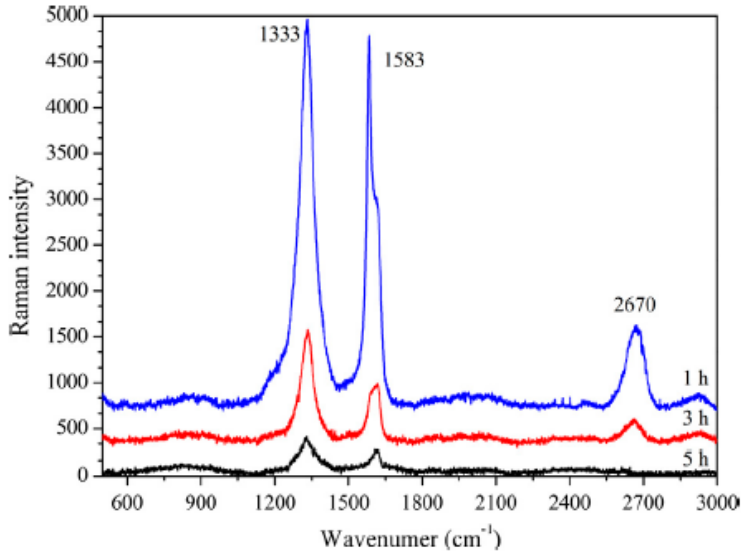

Fig. 2. Secondary electron SEM micrograph of the multilayered morphology of graphene nanoplatelets. (a) 1A, (b) 5A, (c) 1D and (d) 5D.

and single walled carbon nanotubes (SWCNTs) has been previously been studied [13] ; [14]. It has also been observed that a progressive milling time leads to an amorphization of these carbon allotropes by the introduction of disorder in their structures from the beginning of milling. An amorphous spectrum was obtained in experiments related with graphite and diamond after 5000 h of milling, whilst in the case of SWCNTs the Raman spectra indicates a maximum milling time of 50 h to obtain an amorphous structure. It is important to notice that the previous results were obtained in low energy ball mills. In this concern, GNP/Al spectra displays a similar behavior as a function of milling time to that observed in graphite, diamond and SWCNTs after the milling process in a high energy ball mill. However, it can be

observed that crystallinity in the structure of GNPs incorporated in the composite 5D is presented for 5 h of milling. Even though, amorphous structures can be obtained in a shorter milling time by high energy ball mills in comparison with low energy ball mills. The use of high energy ball mills for the production of GNP/Al composites does not lead to the amorphization of GNPs at 5 h of milling. This could be because GNPs are dispersed in a ductile matrix, and aluminum provides a protection from the constant collisions. This protection during milling delays the formation of amorphous GNPs structures.

Milling time and GNP concentration have an important influence over morphology, powder size, microstructure and physical properties in GNP/Al composites. Fig. 3 shows a comparative analysis for different samples with different milling conditions and GNP concentrations. It is presented the morphology evolution of GNP/Al powder during the milling process as a function of milling time (1 and 5 h) and GNP concentration (0 and 1.0 wt%) in this figure. A visible plastic deformation is observed in several particles, which present a flake-like morphology, in samples 1A and 1D (Fig. 3a and c respectively) after 1 h of milling. The inset for Fig. 3a and c, displays the powder cross-section microstructure of a typical lamellar ductile system after high energy milling. It is important to notice that clusters of GNPs are not visible for 1 h of milling. It indicates an excellent dispersion of the GNPs in the

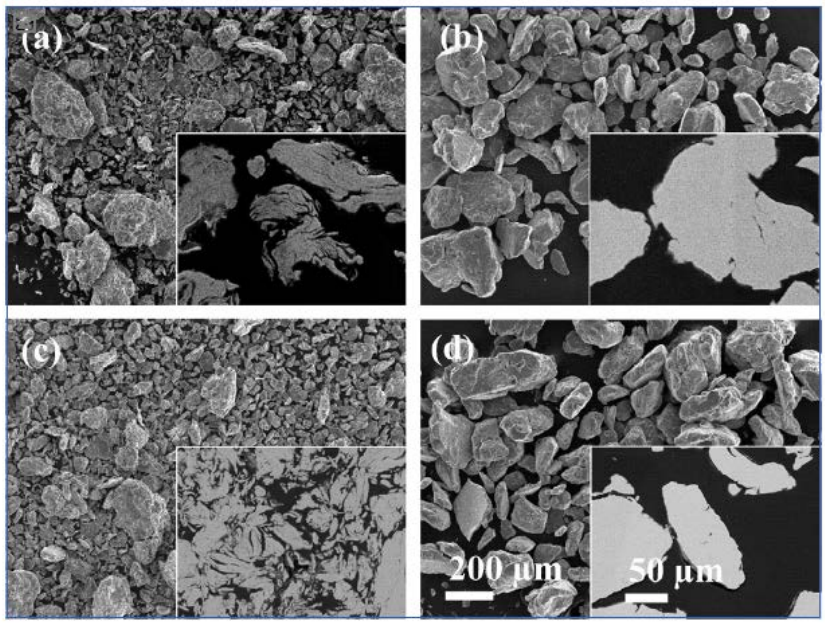

Fig. 3. Raman spectra for aluminum and graphene/aluminum composites (1.0 wt%) for 1, 3 5 h of milling time in the as-milled condition.

aluminum matrix in short periods of milling time by using high energy ball milling. An increase in particle size from 1 h to 5 h of milling time is observed, as a consequence of the increase in the number of impacts of particles by the milling media, which indicates a predominance of the cold welding over the fracture stage during milling process [10] ; [11], giving-rise more equiaxed particles. Particles shown in Fig. 3b exhibited a noticeable reduction in the amount of flattened particles.

The effect of GNP was also screened. The reinforced composite with 1 wt% of GNPs (Fig. 3c) shows a similar behavior of sample 1A (Fig. 3a). A similar case was observed in sample 5D. It can be seen that after 5 h of milling the 5A (Fig. 3b) alloy and the 5D (Fig. 3d) composite present a similar size in their particles, which indicates that a predomination of plastic deformation and cold welding is presented in the A1 alloy for 5 h of milling in a high energy mill. Longer milling times favor the welding process during milling in GNP/Al composites. From this comparative, it is evident that the low GNP added into the aluminum matrix is not enough to have

more evident effect over morphology. The effect of carbon allotropes and milling times on morphology has been reported for CNT/Al composites [12]. In this case, an important effect was observed after longer milling times and high CNT concentrations.

The inset for the 5A and 5D samples show the microstructure after 5 h of milling where, in both cases, the lamellar effect produced by high energy milling process is no longer perceptible, showing homogeneity in the microstructure of the samples. The effect of milling time over microstructural and morphological characteristics in GNP/Al composites is more important than the GNP effect.

SEM micrographs in Fig. 4 show induced fractures in sintered products. The fracture surface corresponds to the 5D composite sintered during 2 h. No clusters of GNPs are observed, which corroborates a homogeneous dispersion according to experimental conditions employed in this research. A ductile fracture is observed which indicates that the concentration of GNP allow a ductile behavior in the composite. The higher GNP concentration employed in this study and the lack of clusters of GNPs suggests good integration in the aluminum matrix and as consequence, a good mechanical bond between GNPs and the aluminum matrix.

Fig. 5 shows X-ray diffraction patterns from the Al and its composites, in the sintered condition. Patterns correspond to the 5A, 5B, 5C and 5D (descending order) after 2 h of sintering. Reflections attained to the carbon element are not presented; this is attributed to the nanometric size and the low content of the reinforcement phase which cannot be detected due to the detection limit presented by XRD for second phases [11]. It can be observed the effect of the chemical reaction between

GNPs with the Al matrix, in the formation of a compound identified as the aluminum carbide Al4C3. The presence of aluminum carbide has been observed in

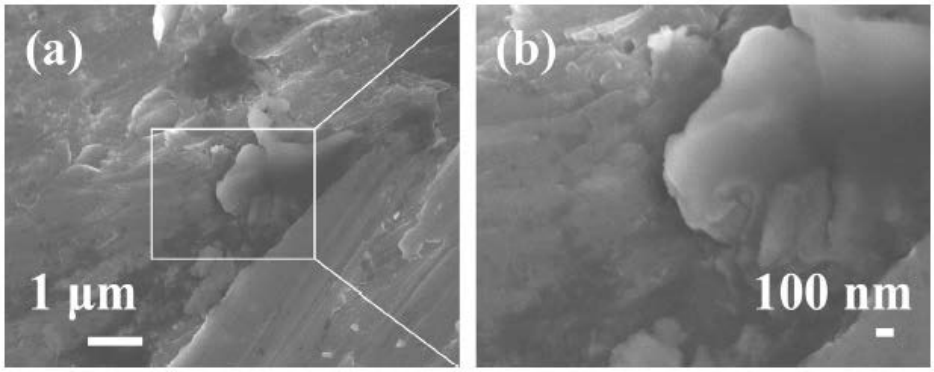

Fig. 4. (a) Fractography of the 5D composite after 2 h of milling. (b) Magnified view of (a).

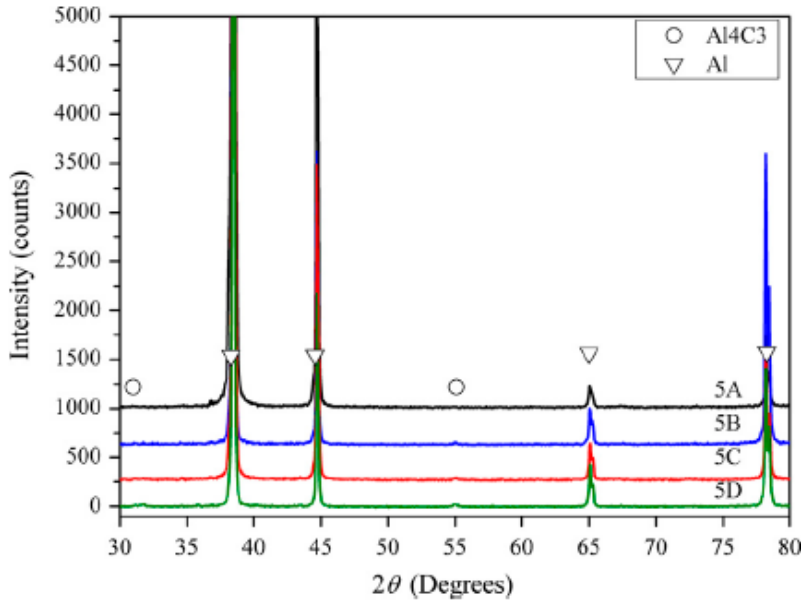

Fig. 5. Patterns of the composites after 2 h of sintering.

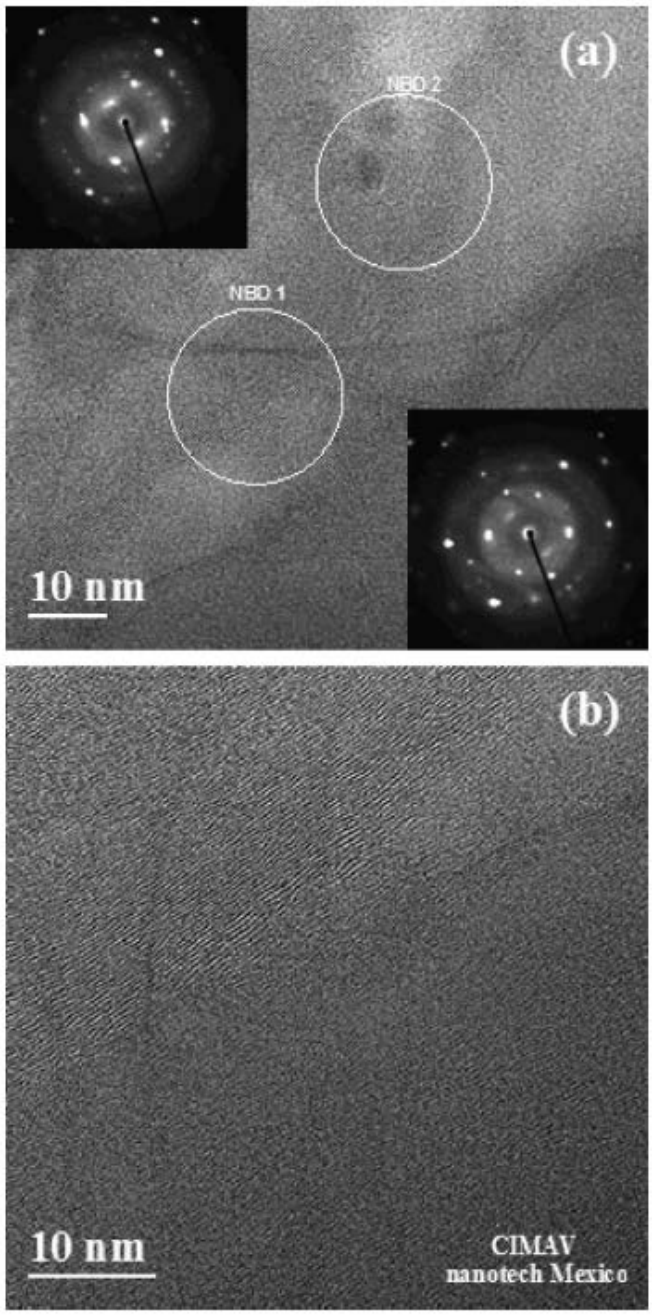

Fig. 6. Bright field TEM micrographs of the 5D composite sintered during 2 h. (a) NBD patterns and (b) HRTEM of the GNPs embedded in the aluminum matrix.

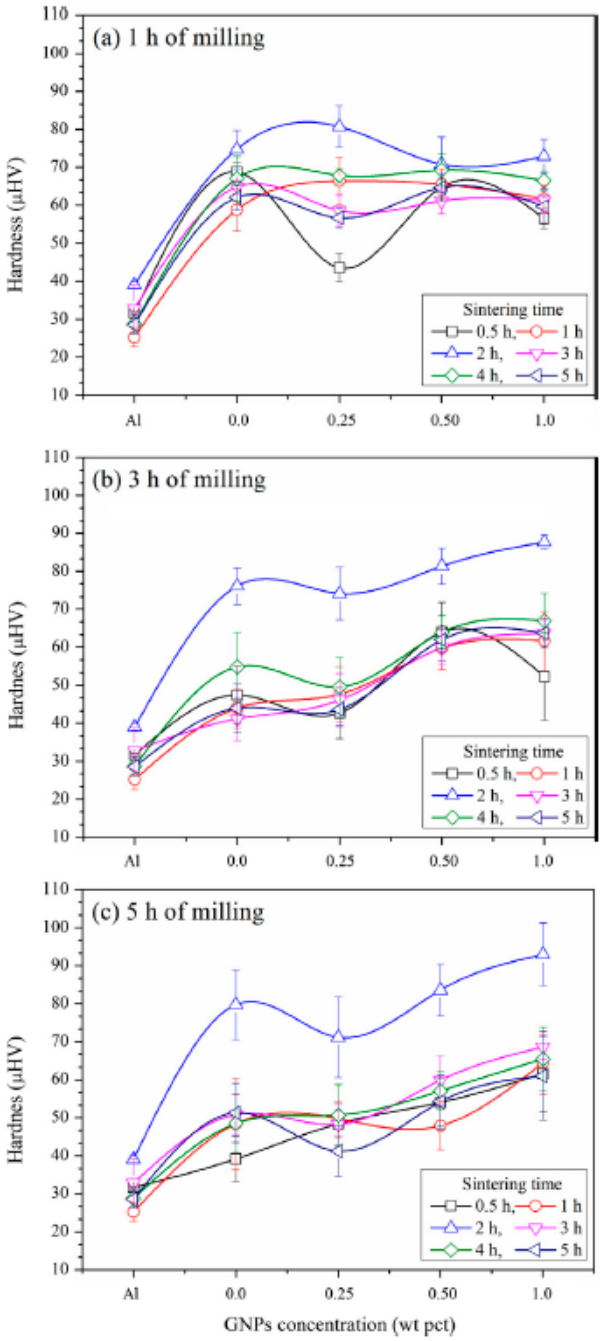

Fig. 7. Vickers micro-hardness results. (a) 1 h, (b) 3 h and (c) 5 h of milling. Pure and not milled aluminum as reference sample is included.

the production of CNT/Al composites synthesized by several routes, where its formation show a strong dependence of the processing temperature followed in the production of the composites [6]. This observation agree with the results obtained by

Bartolucci et al. [4], where they reported the formation of aluminum carbide in graphene/aluminum composites processed by hot extrusion.

Observations by TEM show the crystallinity of GNP as well as the interaction with aluminum matrix. Fig. 6 shows a bright field TEM micrograph of the GNPs embedded in the aluminum matrix. Micrographs were acquired from a 5D sample sintered during 2 h at 500 °C. Nanobeam diffraction (NBD) patterns of two zones are displayed in Fig. 6a. Areas of acquisition are shown with white circles. Even though, crystalline patterns are obtained, halo rings can be observed in the NBD patterns of the selected regions. The result of amorphization of the GNPs agrees with the observations carried out by Raman spectroscopy. An HRTEM micrograph of the platelets–aluminum interphase is displayed in Fig. 6b. It can be noted a transition zone, which indicates intercalation between atoms of carbon and aluminum. The presence of a transition zone indicates a strong aluminum–GNP bond which suggests as a consequence the existence of strengthening mechanisms such as the thermal mismatch between aluminum and GNPs and effective transition layers to transfer load from aluminum to the reinforcement and interaction with dislocations. Such mechanisms have been proposed for the aluminum-based composites reinforced with CNTs [15] ; [16].

Milling time, GNP concentration and sintering conditions have an important effect on mechanical properties. Results from Vickers micro-hardness test are shown in Fig. 7. Micro-hardness results are displayed as a function of milling time and sintering conditions for each milling time: 1 h (Fig. 7a), 3 h (Fig. 7b) and 5 h (Fig. 7c). As a reference, measurements in pure aluminum under the same sintering

conditions are presented. GNPs have a direct relationship and positive effect on hardness. Furthermore, as the milling time increases higher hardness values are observed.

It can be observed that in all cases, higher hardness values were obtained at 2 h of sintering, obtaining the highest values in composites milled for 5 h. For 5 h of milling, the 5D composites present 93 hardness units over the 5A (79 μHV) and the pure aluminum sample (39 μHV), which represent an increase of ~17% and ~138%. The increase in the milling time, in order to produce finer structures, produces harder materials with higher diffusion rates and as a consequence the reduction in the sintering time [11] is presented. As it can be observed, this effect is maximized by the content of GNPs. In this concern, studies about sintering temperature and milling conditions must be further investigated in order to maximize the use of graphene and graphene platelets in the production of aluminum-based composites.

4. Conclusions

• GNP/Al composites were produced by mechanical alloying.

• GNPs were added in concentrations of 0.25, 0.5 and 1.0 wt% and dispersed by milling process at 1, 3 and 5 h of milling.

• Aluminum coat on graphene delayed the formation of amorphous structures in graphene as a consequence of the increase of milling time.

• Milling time and GNPs have a positive effect on hardness values.

• The mechanical behavior of GNP/Al composites evaluated by hardness show that increase in the milling time leads to the production of harder composites at 2 h sintering.

Acknowledgements

Thanks to P. Piza-Ruíz, O. Solis-Canto, W. Antúnez-Flores, C. Leyva-Porras and K. Campos-Venegas for their valuable technical assistance.

References

[1] Y. Wu, G.-Y. Kim, A.M. Russell, Mater. Sci. Eng., A 538 (2012) 164–172.

[2] S. Salimi, H. Izadi, A.P. Gerlich, J. Mater. Sci. 46 (2011) 409–415.

[3] K. Hansang, L. Marc, Nanotechnology 23 (2012) 415701.

[4] S.F. Bartolucci, J. Paras, M.A. Rafiee, J. Rafiee, S. Lee, D. Kapoor, N. Koratkar, Mater. Sci. Eng., A 528 (2011) 7933–7937.

[5] J. Wang, Z. Li, G. Fan, H. Pan, Z. Chen, D. Zhang, Scripta Mater. 66 (2012) 594–597.

[6] R. Pérez-Bustamante, F. Pérez-Bustamante, I. Estrada-Guel, L. Licea-Jiménez, M. Miki-Yoshida, R. Martínez-Sánchez, Mater. Charact. 75 (2013) 13–19.

[7] A. Javadi, S. Mirdamadi, M. Faghihisani, S. Shakhesi, R. Soltani, Fullerenes, Nanotubes, Carbon Nanostruct. 21 (2013) 436–447.

[8] S. Bae, H. Kim, Y. Lee, X. Xu, J.-S. Park, Y. Zheng, J. Balakrishnan, T. Lei, H. Ri Kim,

Y. I. Song, Y.-J. Kim, K.S. Kim, B. Ozyilmaz, J.-H. Ahn, B.H. Hong, S. Iijima, Nat. Nanotechnol. 5 (2010) 574–578.

[9] Y. Zhu, S. Murali, W. Cai, X. Li, J.W. Suk, J.R. Potts, R.S. Ruoff, Adv. Mater. 22 (2010) 3906–3924.

[10] J. Benjamin, Metall. Mater. Trans. B 1 (1970) 2943–2951.

[11] C. Suryanarayana, E. Ivanov, V.V. Boldyrev, Mater. Sci. Eng., A 304–306 (2001) 151–158.

[12] R. Pérez-Bustamante, F. Pérez-Bustamante, I. Estrada-Guel, C.R. Santillán-Rodríguez, J.A. Matutes-Aquino, J.M. Herrera-Ramírez, M. Miki-Yoshida, R. Martínez-Sánchez, Powder Technol. 212 (2011) 390–396.

[13] K. Niwase, T. Tanaka, Y. Kakimoto, K.N. Ishihara, P.H. Shingu, Mater. Trans. JIM 36 (1995) 282–288.

[14] N. Pierard, A. Fonseca, J.F. Colomer, C. Bossuot, J.M. Benoit, G. Van Tendeloo, J.P. Pirard, J.B. Nagy, Carbon 42 (2004) 1691–1697.

[15] R. Pérez-Bustamante, I. Estrada-Guel, W. Antúnez-Flores, M. Miki-Yoshida, P.J. Ferreira, R. Martínez-Sánchez, J. Alloys. Comp. 450 (2008) 323–326.

[16] R. George, K.T. Kashyap, R. Rahul, S. Yamdagni, Scripta Mater. 53 (2005) 1159–1163.